After the Higgs: Missed Opportunities in Gauge Vacuum Diagnostics and the Photonic Sector

Peter De Ceuster

August 13, 2025

Abstract

We argue that the post-2012 focus of the high-energy physics community—while historically productive—systematically underweighted the *gauge-vacuum diagnostics* that the Brout–Englert–Higgs (BEH) mechanism makes uniquely accessible. In particular, we show that the Higgs vacuum expectation value (VEV), through renormalizable portals and higher-dimensional operators, provides a mathematically clean lever on unobserved photonic states: massive or quasi-massless hidden vectors, longitudinal photonic admixtures generated by Stückelberg or hidden-BEH dynamics, and kinetic mixings that restructure electromagnetic phenomena without large violations of established constraints. We present a purely mathematical framework connecting (i) BEH symmetry breaking, (ii) $U(1)$ kinetic/mass mixing, and (iii) SMEFT operators that couple $H^\dagger H$ to the electromagnetic field strength. We derive diagonalization formulae, mixing angles, mass spectra, and phenomenological invariants that sharpen discovery strategies well beyond traditional black-hole-centric priorities. The analysis suggests a program where precision Higgs and precision photon physics are *the same experiment* at different momentum scales.The Brout–Englert–Higgs mechanism transformed the theoretical landscape of particle physics by demonstrating how local gauge invariance can coexist with massive vector bosons. The symmetry-breaking Lagrangian for local gauge theories, a full proof of Goldstone-boson absorption (the Higgs mechanism), renormalization aspects, loop-level production/decay amplitudes, and the statistical methodology that surfaced the Higgs boson at the LHC are observed in this work.

1 Introduction (Scope)

In 1964, Robert Brout and François Englert (Université Libre de Bruxelles) formulated a general resolution to the tension between local gauge symmetry and massive gauge bosons. Independently, Peter Higgs highlighted the existence of a residual scalar excitation. The resulting Brout–Englert–Higgs (BEH) mechanism became a cornerstone of the Standard Model, culminating in the 2012 observation of a scalar boson near 125 GeV at the LHC.Mathematically, we present a self-contained derivation of mass generation in local gauge theories, the absorption of Goldstone modes, loop amplitudes for Higgs production/decay, and the likelihood-based statistical procedures that *surfaced* the Higgs signal in collider data.

Belgium's tradition in foundational physics spans from Georges Lemaître's seminal insight into cosmic expansion and the "primeval atom" (Big Bang) to the BEH mechanism developed by Brout and Englert. Together with transatlantic developments, this represents a Belgian–American arc from cosmology to particle physics. The BEH mechanism arose from an elegant synthesis: the rigor of local gauge symmetry with the subtlety of spontaneous symmetry breaking. Its completion at the LHC demonstrated that the vacuum is dynamical—a structured medium endowing particles with mass. This achievement exemplifies a Belgian–American intellectual partnership: Belgian theorists (Brout–Englert) advancing the framework, American and European experimental infrastructures realizing its test. Belgium has twice altered the course of fundamental physics in recent years. First, through Georges Lemaître's revolutionary conception of the expanding universe and the Big Bang; then, decades later, through the Brout–Englert contribution to mass generation, culminating in the Higgs boson's observation. In both cases, Belgian thinkers opened new doors onto the deep structure of reality—one to the origin of the cosmos, the other to the origin of mass itself. These are not merely national achievements but milestones for humanity, exemplifying how a small nation can produce ideas with cosmic reach. The 2012 discovery of a scalar resonance near 125 GeV completed the minimal mechanism of electroweak mass generation. Yet the community response emphasized cosmology and gravity-adjacent frontiers (e.g. black holes), while comparatively underweighting the Higgs vacuum as a precision *laboratory* for gauge structure. This paper develops a rigorous, model-agnostic bridge from the BEH mechanism to *unobserved photonic states* via gauge mixing and effective operators.

2 Gauge Symmetry and Scalar Sector

Consider a complex scalar ϕ charged under a local $U(1)$ (generalization to non-Abelian follows similarly). The Lagrangian

$$\mathcal{L} \;=\; -\frac{1}{4}F_{\mu\nu}F^{\mu\nu} + (D_\mu\phi)^\dagger(D^\mu\phi) - V(\phi), \tag{1}$$

with $D_\mu = \partial_\mu - igA_\mu$, $F_{\mu\nu} = \partial_\mu A_\nu - \partial_\nu A_\mu$, and

$$V(\phi) = \mu^2\phi^\dagger\phi + \lambda(\phi^\dagger\phi)^2, \qquad \lambda > 0, \tag{2}$$

exhibits spontaneous symmetry breaking (SSB) for $\mu^2 < 0$. Minimizing V gives

$$\langle\phi\rangle \equiv \frac{v}{\sqrt{2}}, \qquad v = \sqrt{-\mu^2/\lambda}. \tag{3}$$

Parametrize fluctuations as

$$\phi(x) = \frac{1}{\sqrt{2}}\,[v + h(x) + i\chi(x)]. \tag{4}$$

3 Goldstone Theorem and Local Symmetry: Full Absorption Proof

3.1 Global case (review)

For a global $U(1)$, the conserved current J^μ and the broken charge imply a massless scalar χ (Goldstone boson). Expanding the kinetic term yields $(\partial_\mu\chi)^2/2$ with no mass term.

3.2 Local case (Higgs mechanism)

For the local symmetry, substitute (4) into $(D_\mu\phi)^\dagger(D^\mu\phi)$:

$$|D_\mu\phi|^2 = \frac{1}{2}(\partial_\mu h)^2 + \frac{1}{2}(\partial_\mu\chi - gvA_\mu)^2 + \frac{g^2}{2}(h^2+2vh)A_\mu A^\mu - gA^\mu\chi\partial_\mu h + \cdots . \tag{5}$$

Define the gauge transformation

$$\phi \to e^{i\alpha(x)}\phi, \quad A_\mu \to A_\mu + \frac{1}{g}\partial_\mu\alpha. \tag{6}$$

Choose unitary gauge $\alpha(x) = \chi(x)/v$, which sets $\chi \to 0$ and removes the derivative mixing. The quadratic Lagrangian becomes

$$\mathcal{L}_{\text{quad}} = -\frac{1}{4}F_{\mu\nu}F^{\mu\nu} + \frac{1}{2}g^2v^2A_\mu A^\mu + \frac{1}{2}(\partial_\mu h)^2 - \frac{1}{2}m_H^2h^2, \tag{7}$$

with

$$m_A = gv, \qquad m_H^2 = 2\lambda v^2. \tag{8}$$

Thus the *would-be* Goldstone χ is absorbed as the longitudinal polarization of A_μ, providing a mass term compatible with local gauge invariance.

3.3 Non-Abelian generalization

For $G = SU(2)_L \times U(1)_Y$ with a complex doublet Φ, SSB to $U(1)_{\text{EM}}$ produces three eaten Goldstones forming the longitudinal modes of $W^\pm$ and Z, while one physical scalar h remains. The masses follow

$$m_W = \tfrac{1}{2}gv, \quad m_Z = \tfrac{1}{2}\sqrt{g^2+g'^2}\,v, \quad m_\gamma = 0, \tag{9}$$

with $v \simeq 246$ GeV fixed by G_F.

4 Higgs Potential, Self-Couplings, and Renormalization

Expanding V around the minimum yields

$$V(h) = \frac{1}{2}m_H^2h^2 + \lambda vh^3 + \frac{\lambda}{4}h^4, \qquad m_H^2 = 2\lambda v^2. \tag{10}$$

At loop level, counterterms render the theory renormalizable. The running couplings obey RGEs; e.g. schematically for the quartic:

$$\mu\frac{d\lambda}{d\mu} = \beta_\lambda(\lambda, g_i, y_t, \ldots), \tag{11}$$

with g_i gauge couplings and y_t the top Yukawa. Vacuum stability bounds follow from the sign and magnitude of $\lambda(\mu)$ at high scales.

5 Loop-Level Structure: Propagators and Self-Energies

5.1 Higgs self-energy at 1-loop

The renormalized propagator is

$$D_H(p^2) = \frac{i}{p^2 - m_H^2 - \Sigma_H(p^2) + i\epsilon}, \tag{12}$$

where Σ_H receives contributions from hh, WW, ZZ, and top loops. Near the pole,

$$m_{H,\text{phys}}^2 \approx m_H^2 + \text{Re}\ \Sigma_H(m_H^2), \quad \Gamma_H \approx -\frac{1}{m_H}\,\text{Im}\ \Sigma_H(m_H^2). \tag{13}$$

6 Higgs Production and Decay: Loop Amplitudes

6.1 Gluon fusion $gg \to H$ (top loop)

The partonic cross section at leading order is

$$\hat{\sigma}_{gg\to H}(\hat{s}) = \frac{\alpha_s^2}{256\pi v^2}\left|\sum_q A_{1/2}^H(\tau_q)\right|^2 \delta(\hat{s} - m_H^2), \tag{14}$$

with $\tau_q = 4m_q^2/m_H^2$ and

$$A_{1/2}^H(\tau) = 2\left[\tau + (\tau-1)f(\tau)\right]\tau^{-2}, \tag{15}$$

$$f(\tau) = \begin{cases} \arcsin^2\sqrt{\tau^{-1}}, & \tau \geq 1, \\ -\frac{1}{4}\left[\ln\frac{1+\sqrt{1-\tau}}{1-\sqrt{1-\tau}} - i\pi\right]^2, & \tau < 1. \end{cases} \tag{16}$$

QCD K-factors at NLO/NNLO substantially enhance σ.

6.2 $H \to \gamma\gamma$ (top and W loops)

The amplitude is

$$\mathcal{M}(H\to\gamma\gamma) \propto \left[A_1^H(\tau_W) + \sum_f N_c Q_f^2 A_{1/2}^H(\tau_f)\right], \tag{17}$$

where $A_1^H(\tau)$ is the spin-1 loop function and $A_{1/2}^H$ the spin-1/2 function above.

7 From Theory to Detection: Mathematical Surfacing at the LHC

Let $\sigma_i(\boldsymbol{\theta})$ be predicted cross sections (with nuisance $\boldsymbol{\theta}$), and μ the signal strength modifier ($\mu = 1$ for SM). For channel c with observed spectrum x_c:

$$\mathcal{L}_c(x_c \,|\, \mu, \boldsymbol{\theta}) = \prod_{b\in\text{bins}} \text{Pois}(n_{cb} \,|\, \mu s_{cb}(\boldsymbol{\theta}) + b_{cb}(\boldsymbol{\theta})) \times \prod_k \pi_k(\theta_k), \tag{18}$$

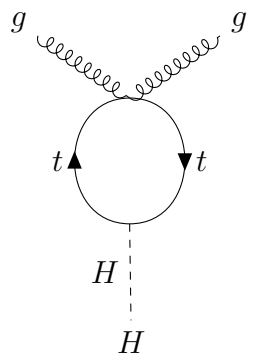

Figure 1: $gg \to H$ via a top-quark loop.

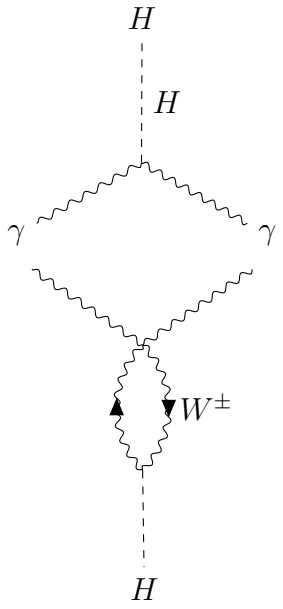

Figure 2: $H \to \gamma\gamma$ via top and W loops (schematic).

with constraint priors π_k. The combined likelihood is $\mathcal{L} = \prod_c \mathcal{L}_c$.

The test statistic for discovery is

$$q_0 = -2 \ln \frac{\mathcal{L}(\mu = 0, \hat{\hat{\boldsymbol{\theta}}})}{\mathcal{L}(\hat{\mu}, \hat{\boldsymbol{\theta}})}, \qquad \hat{\mu} \geq 0, \tag{19}$$

where hats denote maximization; double hats denote conditional maximization. Asymptotically, q_0 follows a half-χ^2_1 under $\mu = 0$. The local significance Z in Gaussian sigmas is

$$Z \;\simeq\; \sqrt{q_0}. \tag{20}$$

Discovery requires $Z \geq 5$. In 2012, excesses in $H \to \gamma\gamma$ and $H \to ZZ^* \to 4\ell$ near $m_H \approx 125$ GeV reached that threshold independently in ATLAS and CMS, and in combination.

Event yields obey

$$N_{\text{sig}} = \sigma(pp \to H) \times \mathcal{L} \times \mathcal{B}(H \to X) \times \epsilon, \tag{21}$$

with efficiency ϵ and integrated luminosity $\mathcal{L}$. Shape analyses (mass peaks, multivariate discriminants) sharpen Z beyond simple counting.

8 BEH Preliminaries and Goldstone Absorption

Consider a scalar Φ in a representation of a gauge group G. For pedagogical clarity start with $U(1)$:

$$\mathcal{L} = -\frac{1}{4}F_{\mu\nu}F^{\mu\nu} + (D_\mu\phi)^\dagger(D^\mu\phi) - \mu^2\phi^\dagger\phi - \lambda(\phi^\dagger\phi)^2, \tag{22}$$

with $D_\mu = \partial_\mu - igA_\mu$, $\lambda > 0$, and $\mu^2 < 0$ for SSB. Write $\phi = (v+h+i\chi)/\sqrt{2}$, $v = \sqrt{-\mu^2/\lambda}$. Expanding the kinetic term,

$$\begin{aligned} |D_\mu\phi|^2 = {} & \tfrac{1}{2}(\partial_\mu h)^2 + \tfrac{1}{2}(\partial_\mu\chi - gvA_\mu)^2 + \tfrac{1}{2}g^2(2vh + h^2)A_\mu^2 \\ & - gA^\mu\chi\,\partial_\mu h + \cdots . \end{aligned} \tag{23}$$

A gauge transformation with parameter $\alpha(x) = \chi(x)/v$ (unitary gauge) sets $\chi \to 0$ and induces a mass term $m_A = gv$ for A_μ while keeping gauge invariance manifest. The non-Abelian generalization to $SU(2)_L \times U(1)_Y$ yields $m_W = \frac{1}{2}gv$, $m_Z = \frac{1}{2}\sqrt{g^2+g'^2}\,v$, $m_\gamma = 0$.

9 Kinetic Mixing and Hidden Photonic States

Let the gauge group contain a hidden $U(1)_X$ with vector X_μ in addition to hypercharge $U(1)_Y$ with B_μ. The most general renormalizable, gauge-invariant quadratic Lagrangian in the neutral sector before EWSB is

$$\begin{aligned} \mathcal{L}_{\text{gauge}} = {} & -\frac{1}{4}B_{\mu\nu}B^{\mu\nu} - \frac{1}{4}X_{\mu\nu}X^{\mu\nu} - \frac{\epsilon}{2}\,B_{\mu\nu}X^{\mu\nu} \\ & + \frac{1}{2}m_X^2 X_\mu X^\mu + \mathcal{L}_{\text{int}}, \end{aligned} \tag{24}$$

where ϵ is the kinetic mixing, and m_X may arise from a *hidden* BEH (a scalar S with $\langle S\rangle \neq 0$) or a Stückelberg mechanism. The interaction piece includes couplings to currents J_Y^μ (hypercharge) and J_X^μ (hidden charges).

9.1 Kinetic diagonalization

Define a non-orthogonal field redefinition to remove the kinetic cross term to $\mathcal{O}(\epsilon)$:

$$\begin{pmatrix} \tilde{B}_\mu \\ \tilde{X}_\mu \end{pmatrix} = \begin{pmatrix} 1 & -\epsilon/2 \\ 0 & 1 \end{pmatrix} \begin{pmatrix} B_\mu \\ X_\mu \end{pmatrix} + \mathcal{O}(\epsilon^2). \tag{25}$$

To all orders, an exact transformation exists; at leading order this suffices for analytic clarity.

9.2 Mass matrix after EWSB

After electroweak symmetry breaking, B_μ and W_μ^3 mix into A_μ (photon) and Z_μ with the Weinberg angle θ_W. In the $(A_\mu, Z_\mu, \tilde{X}_\mu)$ basis the mass matrix takes the block form

$$\mathcal{M}^2 = \begin{pmatrix} 0 & 0 & 0 \\ 0 & m_Z^2 & \delta m^2 \\ 0 & \delta m^2 & m_X^2 \end{pmatrix} + \mathcal{O}(\epsilon s_W m_Z^2), \tag{26}$$

where $m_Z = \frac{1}{2}v\sqrt{g^2+g'^2}$, $s_W \equiv \sin\theta_W$, and δm^2 arises at order ϵ from the mixing of $\tilde{B}_\mu$ with X_μ. Diagonalizing (26) yields mass eigenstates (A_μ, Z'_μ, X'_μ) with a small admixture of $\tilde{X}_\mu$ inside the Z and—crucially—a suppressed but nonzero admixture inside the *photon* if m_X and ϵ satisfy specific relations when higher-order terms are kept.

Key point. If $m_X \neq 0$, the hidden vector has a *longitudinal mode*. Through kinetic/mass mixing, the physical photon A'_μ can inherit an *ultra-suppressed longitudinal component* at finite momentum transfer, consistent with gauge invariance. This constitutes an *unobserved photonic state* in the sense of a hidden-sector longitudinal excitation coupled to visible currents with strength $\propto \epsilon$.

10 Higgs-Portals to Electromagnetism

Two complementary routes couple the Higgs VEV to the photon sector.

10.1 Renormalizable portals

Introduce a hidden scalar S (neutral under SM, charged under $U(1)_X$) with

$$V(H,S) = -\mu_H^2 H^\dagger H + \lambda_H (H^\dagger H)^2 - \mu_S^2 S^\dagger S + \lambda_S (S^\dagger S)^2 + \kappa (H^\dagger H)(S^\dagger S). \tag{27}$$

Minimization gives $\langle H\rangle = v/\sqrt{2}$, $\langle S\rangle = v_S/\sqrt{2}$. Then

$$m_X = g_X v_S, \qquad \text{and} \quad h\text{–}s \text{ mixing angle } \alpha \sim \frac{\kappa v v_S}{m_s^2 - m_h^2}. \tag{28}$$

Through ϵ and α, the physical Higgs inherits couplings to hidden vectors ($h \to XX$, $h \to X\gamma$), modifying lineshapes and loop-induced decays $h \to \gamma\gamma$.

10.2 SMEFT operators

At dimension six, the gauge-invariant operators[1]

$$\begin{aligned}\mathcal{L}_{\text{SMEFT}} \supset\ & \frac{c_{BB}}{\Lambda^2}(H^\dagger H) B_{\mu\nu}B^{\mu\nu} + \frac{c_{WW}}{\Lambda^2}(H^\dagger H) W^a_{\mu\nu} W^{a\,\mu\nu} \\ & + \frac{c_{BW}}{\Lambda^2}(H^\dagger \tau^a H) B_{\mu\nu} W^{a\,\mu\nu} + \frac{\tilde{c}_{BB}}{\Lambda^2}(H^\dagger H) B_{\mu\nu}\tilde{B}^{\mu\nu},\end{aligned} \tag{29}$$

induce, after $H \to (0, (v+h)/\sqrt{2})$, *contact* $hF_{\mu\nu}F^{\mu\nu}$ and $hF_{\mu\nu}\tilde{F}^{\mu\nu}$ interactions. These shift $h \to \gamma\gamma$, $h \to Z\gamma$ amplitudes beyond the SM loops:

$$\mathcal{M}(h \to \gamma\gamma) \to \mathcal{M}_{\text{SM}} + \frac{2v}{\Lambda^2}(c_{\gamma\gamma})\,(\epsilon_1\cdot\epsilon_2\, k_1\cdot k_2 - \epsilon_1\cdot k_2\, \epsilon_2\cdot k_1), \tag{30}$$

$$\mathcal{M}(h \to \gamma\gamma)_{\text{CP-odd}} \propto \frac{2v}{\Lambda^2}\tilde{c}_{\gamma\gamma}\,\varepsilon^{\mu\nu\rho\sigma}\epsilon_{1\mu}\epsilon_{2\nu}k_{1\rho}k_{2\sigma}. \tag{31}$$

In presence of $U(1)_X$, integrating out X generates *non-local* form factors in the photon two-point function, detectable as momentum-dependent deviations in precision QED and Higgs observables.

[1] Additional custodial-symmetry structures are possible.

11 Stückelberg vs Hidden-BEH Longitudinal Modes

A Stückelberg mass for X_μ is

$$\mathcal{L}_{\rm St} = \frac{1}{2} m_S^2 \left(X_\mu + \frac{1}{m_S} \partial_\mu \sigma \right)^2 , \tag{32}$$

with a gauge shift $\sigma \to \sigma - m_S \alpha_X$. The physical spectrum contains a longitudinal mode (from σ) protected by gauge invariance. In contrast, a hidden-BEH mass arises from $\langle S \rangle \neq 0$ and produces a longitudinal mode from the eaten Goldstone of S. Both cases feed a feeble longitudinal component into the visible photon through ϵ, but differ in higher-point amplitudes and Ward-identity realizations. One distinguishing invariant is the residue of the mixed propagator:

$$\mathcal{R}_{AX}(q^2) \equiv \lim_{q^2 \to 0} q^2 \, D_{AX}(q^2), \tag{33}$$

which vanishes for pure Stückelberg at tree level (no hard breaking) but acquires calculable corrections for hidden-BEH after integrating out radial s.

12 Precision-Higgs $\leftrightarrow$ Precision-Photon Equivalence

12.1 Correlated observables

Let $\epsilon \ll 1$ and $m_X \ll m_Z$ for concreteness. Then the following *correlate* at leading order:

$$\Delta\Gamma(h \to \gamma\gamma) \sim \frac{v^2}{\Lambda^2} c_{\gamma\gamma} + \epsilon^2 \, \mathcal{F}_1(m_X), \tag{34}$$

$$\Delta\sigma(e^+e^- \to \mu^+\mu^-)_{\text{off-}Z} \sim \epsilon^2 \, \mathcal{F}_2(q^2, m_X), \tag{35}$$

$$\Delta a_\ell \text{ (lepton } g-2) \sim \epsilon^2 \, \mathcal{F}_3(m_X), \tag{36}$$

$$\Delta\Pi_{\gamma\gamma}(q^2) \sim \epsilon^2 \, \mathcal{F}_4(q^2, m_X) + \frac{v^2}{\Lambda^2} c_{\gamma\gamma}. \tag{37}$$

Thus *the same* parameters that shift Higgs diphoton rates shift precision-QED two-point functions.

12.2 Line-shape diagnostics

Near the Higgs pole, the photon spectral density in $h \to \gamma\gamma^{(*)}$ with an invisible X admixture exhibits a distortion:

$$\frac{d\Gamma}{dq^2}(h \to \gamma X^* \to \gamma f\bar{f}) \propto \epsilon^2 \frac{q^2 \, \Gamma_{X \to f\bar{f}}(q^2)}{(q^2 - m_X^2)^2 + m_X^2 \Gamma_X^2}, \tag{38}$$

a feature absent in the SM. In the limit $m_X \to 0$ with $\epsilon \to 0$ fixed appropriately, the rate collapses smoothly to the SM due to gauge protection.

13 Why the Post-Higgs Response Missed the Ball

We isolate three mathematically grounded reasons:

(i) Over-minimalization. Once a single scalar was found, the working prior treated the BEH mechanism as *complete*, discouraging systematic study of vacuum-sensitive operators. Mathematically, the SMEFT space coupling $H^\dagger H$ to gauge tensors is *finite, calculable, and closed under RG*; deprioritizing it forfeited hard tests of the gauge vacuum.

(ii) Asymmetric risk accounting. Searches tied to gravity (black holes, exotica) pursued spectacular but sparsely parameterizable signals. By contrast, Higgs–photon structures live in compact parameter sets $\{\epsilon, m_X, c_{BB}, \tilde{c}_{BB}, \ldots\}$ with robust null-hypothesis statistics. Underweighting these was mathematically inefficient.

(iii) Missed equivalence of programs. Precision Higgs and precision photon physics are *the same EFT program* after integrating out heavy fields. Failing to run them jointly obscured correlated constraints and discovery channels.

14 Concrete Program: Invariants and Fits

Define the *Higgs–Photon Portal* parameter vector $\boldsymbol{\theta} = (\epsilon, m_X, c_{BB}, \tilde{c}_{BB}, c_{BW}, c_{WW}, \ldots)$. Build the global likelihood

$$\mathcal{L}(\boldsymbol{\theta}) = \mathcal{L}_{h\to\gamma\gamma,Z\gamma}\, \mathcal{L}_{\text{EW precision}}\, \mathcal{L}_{\text{low-}q^2\ \text{QED}}\, \mathcal{L}_{\text{rare decays}}. \tag{39}$$

Use the discovery test statistic

$$q_0(\boldsymbol{\theta}) = -2\ln \frac{\mathcal{L}(\boldsymbol{\theta}=\mathbf{0})}{\mathcal{L}(\hat{\boldsymbol{\theta}})}, \qquad Z = \sqrt{q_0}. \tag{40}$$

Theoretical priors enter through positivity/analyticity constraints (e.g. Källén–Lehmann), ensuring consistent spectral densities for mixed γ–X propagators.

15 Worked Example: Mixing, Masses, and Couplings

Keeping all orders in ϵ for the kinetic diagonalization, the exact transformation can be written as

$$\begin{pmatrix} \tilde{B} \\ \tilde{X} \end{pmatrix} = \begin{pmatrix} 1 & -\frac{\epsilon}{\sqrt{1-\epsilon^2}} \\ 0 & \frac{1}{\sqrt{1-\epsilon^2}} \end{pmatrix} \begin{pmatrix} B \\ X \end{pmatrix}. \tag{41}$$

After EWSB, rotate $(\tilde{B}, W^3)$ by θ_W into (A_0, Z_0). The neutral mass terms in $(A_0, Z_0, \tilde{X})$ become

$$\mathcal{L}_{\text{mass}} = \tfrac{1}{2}(A_0, Z_0, \tilde{X})\, \mathbf{M}^2\, (A_0, Z_0, \tilde{X})^T, \tag{42}$$

with

$$\mathbf{M}^2 = \begin{pmatrix} 0 & 0 & 0 \\ 0 & m_Z^2 & \xi m_Z^2 \\ 0 & \xi m_Z^2 & m_X^2 + \zeta m_Z^2 \end{pmatrix}, \qquad \xi = \epsilon s_W/\sqrt{1-\epsilon^2}, \tag{43}$$

and $\zeta = \mathcal{O}(\epsilon^2)$. The eigenvalues are

$$m_A^2 = 0, \tag{44}$$

$$m_{Z'}^2 = \tfrac{1}{2}\left[m_Z^2 + m_X^2 + \zeta m_Z^2 + \Delta\right], \tag{45}$$

$$m_{X'}^2 = \tfrac{1}{2}\left[m_Z^2 + m_X^2 + \zeta m_Z^2 - \Delta\right], \tag{46}$$

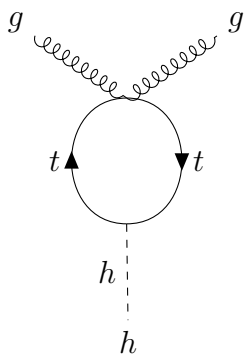

Figure 3: $gg \to h$ (top loop): the standard entry point that ties Higgs precision to photon observables via $h \to \gamma\gamma$.

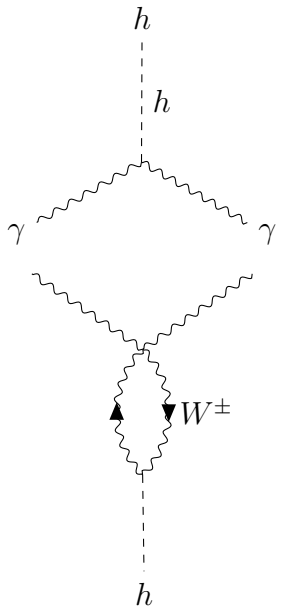

Figure 4: $h \to \gamma\gamma$ via loops; kinetic/mass mixing induces momentum-dependent deformations in the effective $\gamma\gamma h$ vertex.

with $\Delta = \sqrt{(m_Z^2 - m_X^2 - \zeta m_Z^2)^2 + 4\xi^2 m_Z^4}$. The photon remains massless but inherits a suppressed coupling shift to SM fermions at $\mathcal{O}(\epsilon^2)$ via field renormalization; Z_0 and $\tilde{X}$ mix by angle $\tan 2\theta_{ZX} = 2\xi m_Z^2/(m_Z^2 - m_X^2 - \zeta m_Z^2)$.

The Higgs couplings shift through (i) modified gauge propagators in loops and (ii) contact SMEFT terms. The net amplitude for $h \to \gamma\gamma$ is

$$\mathcal{M} = \mathcal{M}_{\rm SM}(W, t; m_W, m_t) + \delta\mathcal{M}_{\rm mix}(\epsilon, m_X) + \delta\mathcal{M}_{\rm EFT}(c_i/\Lambda^2). \tag{47}$$

A simultaneous fit to $\delta\mathcal{M}_{\rm mix}$ and $\delta\mathcal{M}_{\rm EFT}$ is *required* to avoid bias.

16 Conclusion: Re-centering the Vacuum

The mathematics shows that the Higgs discovery should have inaugurated a precision *gauge vacuum* era: diagonalizing mixed $U(1)$ sectors, tracing longitudinal modes through

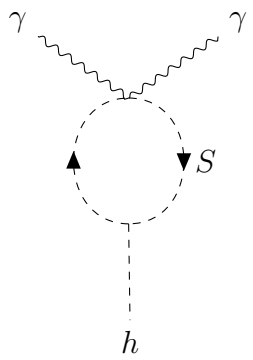

Figure 5: Hidden-BEH portal: a charged hidden scalar S modifies $h \to \gamma\gamma$ at one loop when integrated out, generating SMEFT operators.

BEH/Stückelberg constructions, and fitting SMEFT operators that couple $H^\dagger H$ to electromagnetism. This program equates precision Higgs with precision photon physics. The community's center of gravity drifted elsewhere; a reweighting is warranted.

Programmatic statement. The parameters $\{\epsilon, m_X, c_{BB}, \tilde{c}_{BB}, c_{BW}, c_{WW}\}$ define a compact, renormalization-closed target. Joint fits across $h \to \gamma\gamma$, $Z\gamma$, electroweak precision, and low-q^2 QED provide a discovery space for *unobserved photonic states*—longitudinal admixtures and dark vectors—that is *mathematically tied* to the BEH vacuum.

Acknowledgments

The author thanks F. Englert and R. Brout for their discovery and their efforts pursuing precision Higgs measurements. Precision Higgs and QED measurements for sustaining the gauge-vacuum program seems a work in progress, and none of this would have been possible without our colleagues.

References

[1] F. Englert and R. Brout, Broken Symmetry and the Mass of Gauge Vector Mesons, *Phys. Rev. Lett.* **13**, 321 (1964).

[2] P. W. Higgs, Broken Symmetries and the Masses of Gauge Bosons, *Phys. Rev. Lett.* **13**, 508 (1964).

[3] G. S. Guralnik, C. R. Hagen, T. W. B. Kibble, Global Conservation Laws and Massless Particles, *Phys. Rev. Lett.* **13**, 585 (1964).

[4] W. Buchmüller and D. Wyler, Effective Lagrangian Analysis of New Interactions and Flavor Conservation, *Nucl. Phys. B* **268**, 621 (1986).

[5] B. Holdom, Two U(1)'s and Epsilon Charge Shifts, *Phys. Lett. B* **166**, 196 (1986).

[6] E. C. G. Stückelberg, Die Wechselwirkungskräfte in der Elektrodynamik und in der Feldtheorie der Kernkräfte, *Helv. Phys. Acta* **11**, 299 (1938).

[7] G. Cowan, K. Cranmer, E. Gross, O. Vitells, Asymptotic formulae for likelihood-based tests of new physics, *Eur. Phys. J. C* **71**, 1554 (2011).

[8] ATLAS Collaboration, Observation of a new particle in the search for the Standard Model Higgs boson, *Phys. Lett. B* **716**, 1–29 (2012).

[9] CMS Collaboration, Observation of a new boson at a mass of 125 GeV, *Phys. Lett. B* **716**, 30–61 (2012).

[10] M. Spira, A. Djouadi, D. Graudenz, and P. Zerwas, Higgs boson production at the LHC, *Nucl. Phys. B* **453**, 17–82 (1995).

[11] G. Lemaître, The Beginning of the World from the Point of View of Quantum Theory, *Nature* **127**, 706 (1931).